Challenges in Optimising and Controlling the Electrolyte in Aluminium Smelters

- by Mark P. Taylor

1. THE HALL-HÉROULT ELECTROLYTE

Cryolite, or sodium aluminium hexafluoride, is the basis of the molten salt mixture which has been used to smelt aluminium electrolytically for the past hundred years. This is because cryolite is the only electrically conducting solvent capable of dissolving significant quantities of alumina - this occurs at over 1000°C however. Aluminium fluoride and other salts have been added to cryolite in order to reduce the melting point and therefore the operating temperature of the electrolyte. Over the last forty years the level of aluminium fluoride additive in particular has increased from 3 - 4 wt % to up to 15 wt %, in excess of the cryolite composition, at some smelters. This progression is shown schematically on the sodium fluoride - aluminium fluoride phase diagram in Figure 1 (taken from [1]). The diagram also shows the following important features of the system:

- The liquidus temperature of cryolite-based electrolytes can be reduced to less than 800°C by the addition of large quantities of aluminium fluoride.

- The rate of change of liquidus temperature with AlF_3 composition increases as excess AlF_3 wt % increases from 0 up to 20 - 30 wt %.

- The primary crystallising phase for industrial electrolytes is cryolite. If the excess AlF_3 composition were to exceed 32 wt %, chiolite ($5NaF : 3AlF_3$) or AlF_3 itself would be the crystallising phase.

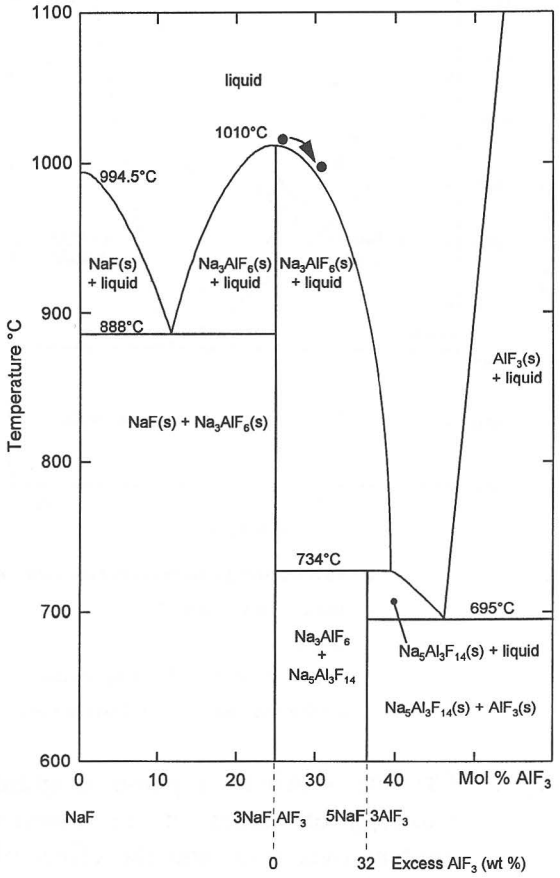

Fig. 1. Sodium Fluoride - Aluminium Fluoride phase diagram showing cryolite and chiolite phases and the change in AlF_3 content over the recent past.

As aluminium fluoride concentration has risen over time, the importance of controlling alumina concentration has increased. The reason for this is shown in another binary section of the electrolyte phase diagram in Figure 2 (from [2]). Alumina solubility is defined by the right-hand liquidus line in Figure 2, and the intersection of this line with the left-hand liquidus line is called the double solubility or pseudo-eutectic point.

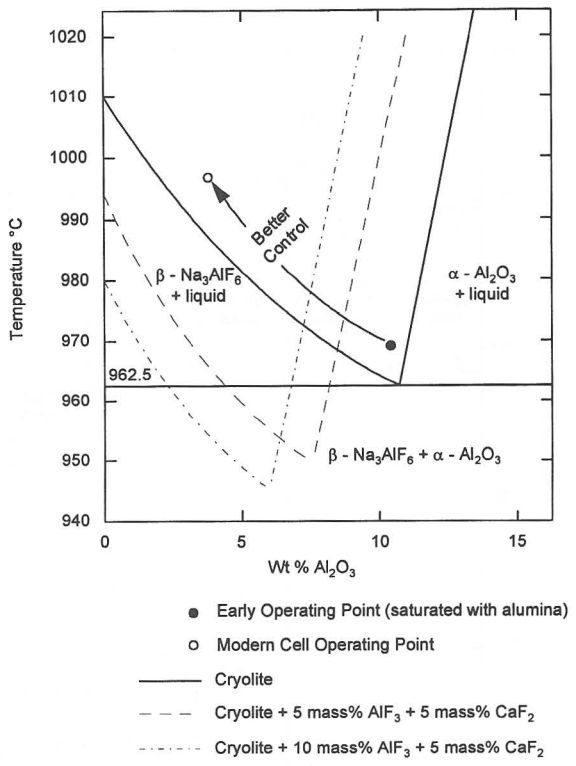

Fig. 2. Cryolite - Alumina phase diagram showing the reduction in alumina content over time and the effect of increasing AlF_3 content on the pseudo-eutectic or 'double solubility' point, from [2].

When the alumina concentration approaches the double solubility point, the concentration driving force for dissolution of added alumina is very small, causing poor dissolution and large scale sludge formation on the bottom of the cell. Sustainable electrolysis therefore requires that the alumina concentration is kept well below this level. This is particularly important at higher aluminium fluoride concentrations because undissolved alumina sludge can freeze onto the cathode - causing magnetohydrodynamic instability in the cell. Sludge solidification is discussed later in this paper.

Figure 2 shows that the solubility of alumina reduces rapidly as aluminium fluoride concentration increases. Better alumina feeding techniques and computer control have enabled alumina concentration control between 2 wt % and 4 wt % for most of the time. However complete depletion of alumina, and resulting electrolysis of fluoride components in the electrolyte (anode effect) still occurs even on point fed smelting cells once or twice every ten days.

The effect of lithium fluoride addition to the electrolyte is shown in Figure 3, calculated from Sterten [15], on the same binary section as used in Figure 2. It is evident that this additive also reduces the operating temperature and alumina solubility of the electrolyte. Lithium fluoride, however, has the advantage of increasing the electrical conductivity of the electrolyte - counteracting the effect of aluminium fluoride which reduces conductivity. Unfortunately lithium fluoride is also co-deposited with aluminium and can be difficult to retain within the electrolyte, due to its rate of loss in the aluminium and high diffusion rate into the cathode. Lithium components are also volatilised from the electrolyte surface, and must be recovered and recycled in order to be economic as an additive.

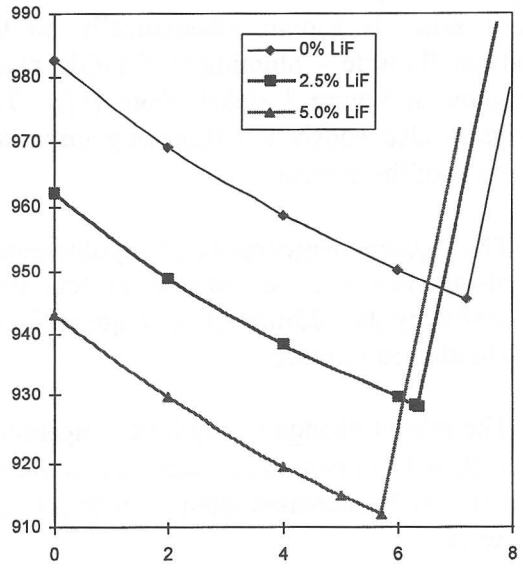

Fig. 3. Effect of LiF Addition on cryolite - AlF_3 - Al_2O_3 System. Excess AlF_3 concentration is 10 wt %. Calculated from Sterten [15].

The rationale for increasing aluminium fluoride concentration is strengthened in Figure 4 where the reduction in aluminium metal solubility with excess aluminium fluoride concentration is shown. Aluminium metal back-reacts with carbon dioxide produced at the anode, causing major losses in current efficiency in the process as described in the next section. High aluminium fluoride concentration counteracts this process somewhat (Figure 4) but can also have serious consequences for the controllability of the electrolyte. The reasons for this and the impact on cell operation and control will be discussed later in the paper.

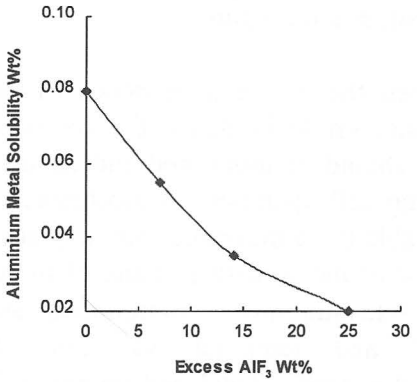

Fig. 4. Aluminium metal solubility in cryolite as a function of AlF_3 addition. Aluminium solubility has been halved since aluminium fluoride addition first started.

2. SMELTING CELL OPERATION

2.1 Anode - Cathode Distance

The smelting process is a horizontal electrode, high current density (0.7 - 1.2 A/cm^2) electrolysis which operates with a liquid aluminium pad accumulating above a carbon cathode. The liquid aluminium forms the cathodic surface and 4 - 5 cm above it are downward facing, consumable carbon anodes. The cell geometry is shown schematically in the cross-sectional view in Figure 5, along with the electrical current path through the cell.

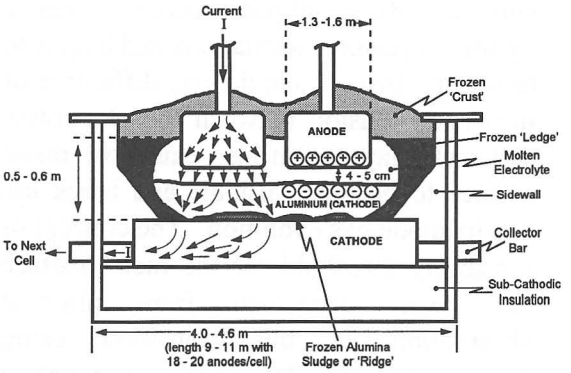

Fig. 5. Schematic representation of an aluminium smelting cell, showing major components and the passage of current from anode to cathode in the cell.

The interpolar distance, or anode-cathode distance (ACD), is destabilised in several ways during operation:

- Vertical components of the magnetic field generated by current flow in the cell conductors can interact with horizontal currents in the aluminium pad - causing transient forces and waves in the metal surface. This phenomenon is less common in magnetically compensated smelters but still occurs if sections of the cathode become covered with solidified alumina/cryolite sludge, when the electrolyte temperature is too low, or when the alumina concentration in the electrolyte is allowed to approach saturation. The reasons for these events are discussed later.

- Carbon dioxide accumulates and coalesces under the anodes as a consequence of the reaction between carbon and oxygen containing anions:

$$C_{(anode)} + 2\,O^{2-} = CO_2 + 4e^- \quad (1)$$

By the time these bubbles are released from the edges of the anodes, they are large

enough to cause significant pressure fluctuations in the electrolyte and disturb the metal surface. Then at low ACD, the surface of the metal pad becomes disrupted by these pressure fluctuations and begins to break up. Insufficient density difference or interfacial tension between the electrolyte and metal layers can also cause the metal surface to become unstable and break up, due to anode gas evolution. The concept of a stability threshold for the metal surface has been formulated from physical observation of this transition using dynamically similar, low temperature fluids to represent the electrolyte and metal. Zhang et al [3] quantified the instability transition which is shown schematically in Figure 6.

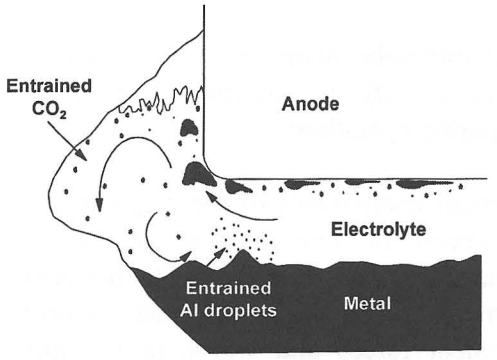

Fig. 6. Electrolyte/Metal interfacial break-up can occur under some conditions due to carbon dioxide gas bubble release from under the anodes. Substantial loss of current efficiency results if interfacial break-up occurs in a cell.

The qualitative conclusions are as follows:

- Increasing electrolyte density and gas/electrolyte interfacial tension both increase the tendency towards metal surface instability.

- Increasing electrolyte viscosity and electrolyte/metal interfacial tension both reduce the tendency towards instability.

- Low ACD, high electrolyte immersion of the anodes, and high local anodic current density (> 1.5 A/cm^2) all increase the tendency towards instability and all show distinct transition points between stable and unstable interface behaviour.

- The faradaic efficiency of the electrolysis will vary by only ± 1 - 2% when there is a stable metal interface and no short circuiting of current between the anodes and metal pad. Under these conditions, efficiencies in excess of 96% are likely to occur.

- Under unstable interface conditions, faradaic efficiency losses of 5 - 10% will occur, as a minimum.

Given the above dependence of faradaic efficiency on ACD, this is the key parameter which should be monitored and controlled in smelting cell operation. Unfortunately ACD is not able to be measured routinely at present because of the corrosive nature of the molten electrolyte/aluminium environment and the spatial and temporal variation of the parameter itself. Total cell potential drop is measured continuously at all aluminium smelters, for the purpose of providing a rudimentary control of anode - cathode distance. Of the 4.2 - 4.7 V total cell potential, between 0.8 - 1.0V is lost through the resistance of the cell anodes, cathode and the associated connections to the aluminium bus bars which take the current from one cell to the next in the series circuit.

The reversible decomposition potential for the cell reaction:

$$\tfrac{1}{2}\, Al_2O_3\,(s) = \tfrac{3}{4}\, C(s) = Al_{(l)} + \tfrac{3}{4}\, CO_2(g) \quad (2)$$

requires another 1.25V, although this value increases at very low alumina concentrations in the electrolyte, as described originally by Rolin [4].

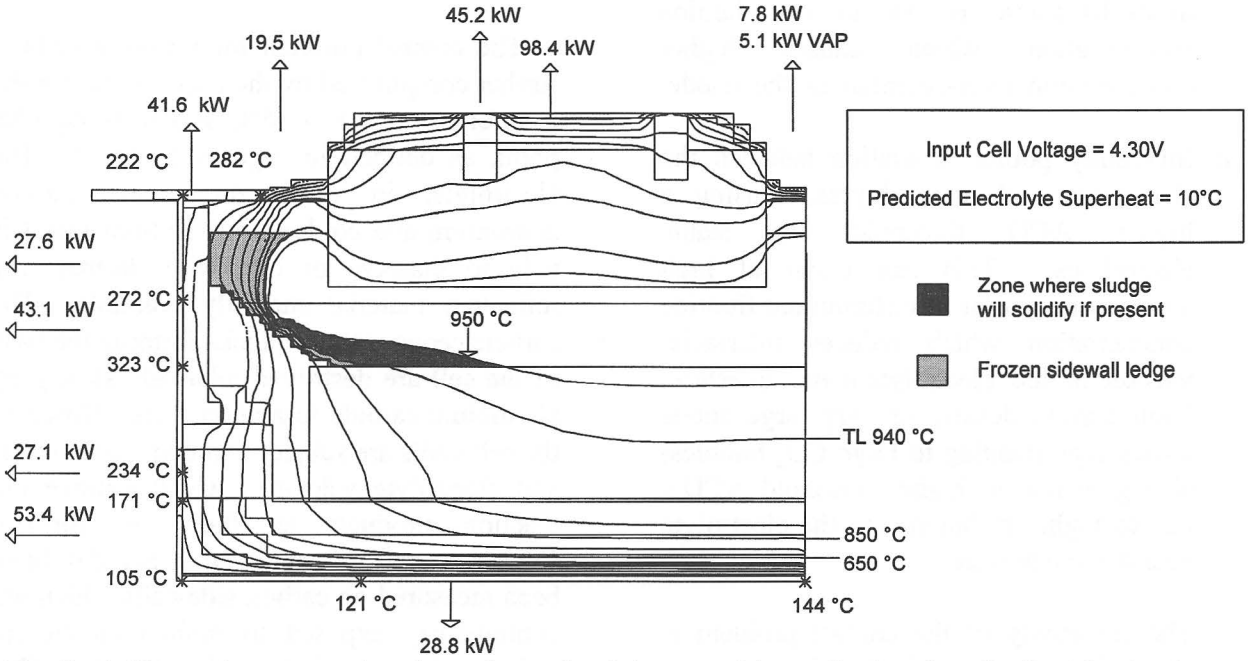

Fig. 7. A Thermal cross-section through an aluminium smelting cell, showing the liquidus isotherm, (940°) defining the cryolite-based ledge on the sidewall, and the 950°C isotherm, below which alumina/cryolite sludge can solidify.

The remaining 2.1 - 2.4V of cell potential is generated within the electrolyte, and at the electrolyte/anode or electrolyte/aluminium interfaces dues to anode and cathode over-potentials respectively. Due to its relatively low electrical conductivity, the passage of current across the anode - cathode distance drives 75% of this potential drop directly. In the case of a modern 180,000 ampere cell operating with an anodic current density of 0.85 A/cm^2 and an anode - cathode distance of 4.5 cm, the ohmic voltage drop across the electrolyte is approximately 1.7V. This drop generates heat which keeps the electrolyte molten and above its liquidus point. The stability of this energy input is crucial to the energy balance of the whole smelting cell, as shown in the steady-state thermal cross-section in Figure 7. The heat input to the electrolyte dominates the generation / dissipation balance and determines the superheat of the electrolyte above its liquidus point. Sidewall ledge thickness, anode and cathode temperatures and top crust mechanical stability are all driven by this balance and the way it changes over time.

The above discussion demonstrates that both the faradaic efficiency of the electrolytic process and the energy balance of the cell are inextricably linked to the ACD. In control terms therefore, once the cell is designed and built, the system is over-determined. A certain heat input is required to provide a superheated electrolyte within a given, insulated cell cavity - the heat dissipation in the ACD is therefore basically fixed. If this heat dissipation corresponds to a physical anode - cathode distance which is below the threshold for stable electrolysis, an unstable and inefficient electrolytic performance will be obtained. This situation can occur due to:

a) Low electrical conductivity of the electrolyte, due to low temperature, high aluminium fluoride concentration or other electrolyte additives.

b) High anode current density, due to high current or lower than required anode cross-section.

c) Low anode - cathode distance, due to either a) or b) above, or due to low alumina concentration which causes higher concentration over-potential at the anode.

d) Inherently poorer separation between the electrolyte and metal layers, causing a higher ACD threshold for stable electrolysis. This can occur at high temperature and/or low aluminium fluoride concentration which reduces interfacial tension at the electrolyte/metal interface. High current density or very large anode dimensions (leading to large CO_2 bubbles) also give rise to higher threshold ACD's due to higher turbulence in the electrolyte near the anode edges.

The sensitivity of the control problem is epitomised by the effect of increasing aluminium fluoride content:

An increase in excess AlF_3 concentration from 9 wt % to 14 wt %, with accompanying reduction in operating temperature from 970°C to 945°C, causes a reduction in electrolyte conductivity from 2.36 $\Omega^{-1}cm^{-1}$ to 2.19 $\Omega^{-1}cm^{-1}$. Under a constant anode - cathode distance control strategy the 180,000 cell discussed earlier would have its electrolyte ohmic potential drop increased by 0.13V or 8%. Heat generation would increase by 23.4 kW in the ACD region, causing over-heating of the electrolyte and melting of the frozen cryolite ledge which protects the sidewall in Figure 7. Using a constant cell potential strategy, however, the control system would act to reduce ACD so that the total potential drop remains the same. A 3 - 4 mm reduction in ACD would occur in this case and a loss of faradaic efficiency may or may not occur depending on the proximity of individual anodes to the molten aluminium surface.

2.2 Electrolyte Phase Change

The control problem for smelting cells is further complicated by the need to operate the electrolyte only 5 - 15°C above its liquidus point, as defined in Figures 1 and 2. The electrolyte, in combination with molten aluminium and co-deposited sodium metal is able to dissolve or otherwise destroy any refractory material currently available. The carbonaceous cathode blocks forming the base of the cell are destroyed relatively slowly by aluminium carbide formation there. However the cell walls are subject to much higher metal and electrolyte velocities which remove the reaction products as they are formed. Corrosion rates of up to 2mm per day have been measured on carbon sidewalls which are continuously exposed to molten electrolyte and metal in an industrial cell [5]. This corrosion process has in the past reduced cell life in some smelters to less than half the normal life of 5 - 6 years.

The design of thin sidewall cells over the past 15 years has significantly reduced this problem by freezing a protective layer of cryolite, called 'ledge', onto the inside face of the walls. At its narrowest point the ledge is only 2 - 3cm thick, however, and an increase in electrolyte superheat above 10 -15°C will generally melt this layer and cause the corrosion process to become active.

This maximum superheat constraint imposed by the need to maintain sidewall ledge causes the electrolyte to be susceptible to freezing in other, less desirable circumstances:

- Quench freezing of electrolyte occurs around newly positioned anodes to the extent of 100 - 200 kg per square metre of anode area, causing a disruption to the flow of current to the anode which may last 24 hours [6].

- Freezing around added alumina powder occurs during feeding of this raw material. If the alumina is not well dispersed, freezing can delay its dissolution in the electrolyte to such an extent that alumina/cryolite aggregates sink beneath the aluminium pad to form a two phase mixture known as sludge [7].

The composition of the electrolyte phase which forms 60% of the sludge layer in smelting cells is different to that of the bulk electrolyte above the aluminium pad. Freezing and partial remelting of the sludge causes rejection of the aluminium fluoride component, leaving alumina-saturated cryolite with some calcium fluoride and a small amount of excess aluminium fluoride [7] as the liquid part of the sludge mixture beneath the metal. In smelters where large amounts of alumina are fed into the electrolyte at a time, the mass of sludge on the cathode is in the order of tonnes - sometimes coming close to the mass of the bulk electrolyte itself.

Since the liquid component of this sludge layer is approximately 10 wt % alumina, and is being gradually fed back into the bulk electrolyte, the control of alumina concentration in cells with high sludge levels is rendered extremely difficult because the rate of alumina feeding cannot be related to the rate of electrolysis. In addition the metal circulation pattern may cause sludge to build up under one or more of the anodes, eventually leading to direct contact between the anode and the sludge - this rapidly over-heats both the anode and the rest of the cell due to the formation of aluminium carbide and sodium metal under the anode. Massive loss of faradaic efficiency results during abnormalities such as this.

Even small amounts of sludge in point-fed cells have been shown to impose a constraint on the operation of the electrolyte however. In Figure 8 (from [7]) a schematic of the pseudo-binary section of the electrolyte liquidus surface (from Figure 2 earlier) is compared with the liquidus point of the electrolyte in sludge.

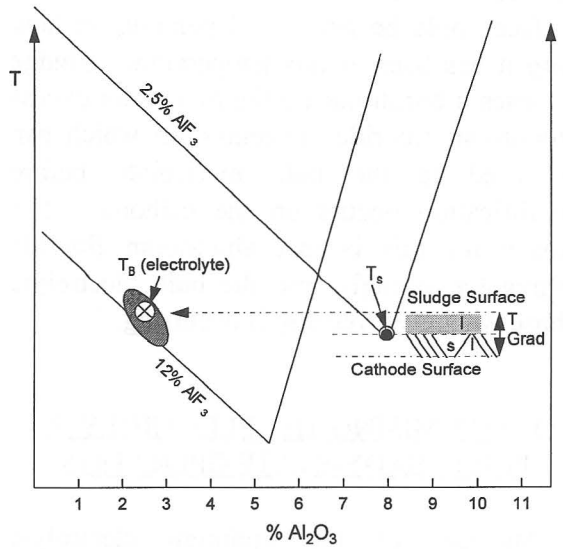

Fig. 8. Schematic showing the solidification point of the cryolite phase in sludge, relative to the operating temperature of the bulk electrolyte above the aluminium layer. Higher AlF_3 content in the electrolyte can result in freezing of the sludge layer - as shown in Figure 7.

The high cryolite content of the sludge causes its liquidus line to be above that of the bulk electrolyte. In fact, because of its alumina saturation and in the absence of lithium fluoride or magnesium fluoride, the sludge freezing point is almost invariant, ranging between 945 - 950°C only. It is evident that if the operating temperature of the bulk electrolyte falls beneath the sludge freezing point, the liquid portion of the sludge will, in time solidify, insulating large sections of the cathode surface against normal electrical current flow, and causing disruption of the current distribution within the aluminium pad. This is the commonest cause of aluminium pad instability as mentioned in Section 2.1.

The position of the 950°C isotherm is plotted in Figure 7 to demonstrate how close a

cell with normal energy balance and electrolyte composition is to freezing sludge onto the cathode. In Figure 7 all sludge lying between the 950°C isotherm and the cathode surface could be frozen - depending on how long it has been at this temperature. Sludge imposes a constraint on the maximum excess aluminium fluoride concentration which can be used in the bulk electrolyte before solidification occurs on the cathode. The reason for this is that aluminium fluoride segregates strongly into the bulk electrolyte phase whenever freezing is occurring.

3. OPTIMISING THE ELECTROLYTE FOR STEADY-STATE OPERATION

Analyses of the optimum electrolyte composition for smelting have been performed previously by Haupin [8, 9]. Table I, by Haupin, is a useful qualitative overview of the main electrolyte property trends with composition. It should be noted, however, that more recent measurements by Fellner et al [10] on viscosity trends with lithium fluoride concentration show that this property actually increases with lithium fluoride content at high excess aluminium fluoride concentrations.

The above analyses sought to answer the question:

"What single electrolyte composition will provide the lowest potential drop in the ACD, with highest faradaic efficiency, and with the lowest total electrolyte losses from the cell?"

Thus high electrical conductivity, high alumina solubility and low electrolyte density are favoured because this should produce a low, stable potential drop in the ACD. Similarly the faradaic efficiency would be maximised by low aluminium solubility and diffusivity within the electrolyte and by the maximum electrolyte/aluminium interfacial tension and high electrolyte viscosity.

To complete this scenario, a low electrolyte vapour pressure reduces losses from the top of the cell into the fume collection ducting, while low diffusion rate of electrolyte components into the cathode also reduces these losses. The advent of fume recycling by alumina dry scrubbing, and the manufacture of graphic and graphitized cathode blocks respectively, have effectively removed these latter constraints on the optimum electrolyte however.

These rather obvious steady state optimisation criteria contain an underlying assumption: that the electrolyte can be operated at a single point in the composition-temperature space. However, control of anode - cathode distance, alumina concentration and electrolyte phase change do not allow this assumption to be applied in practice. Specifically, we must recognise that dynamic criteria such as the stability of the electrolyte composition, the need to maintain the electrodes free from frozen electrolyte and sludge, and the maintenance of a hydrodynamically stable electrolyte /aluminium interface are the basis for a practical optimisation of the industrial smelting electrolyte.

Table I. Properties of molten cryolite with additives.

	Al_2O_3 solub.	Elect. cond.	Density	Visc.	Liq. temp.	Metal solub.	Surf. tens.	Vapour press.
CaF_2	↓	↓	↑	↗	↓	↓	↑	↓
AlF_3	↓	↓	↓	↓	↘	↓	↓	↑
LiF	↓	↑	↑	↓	↓	↓	↑	↓
MgF_2	↓	↓	↑	↑	↓	↓	↑	↓
Al_2O_3	–	↓	↓	↗	↓	↓	↘	↓
Temp.	↑	↑	↓	↓	–	↑	↓	↑

4. UNDERSTANDING THE VARIATION

Once it has been accepted that the electrolyte requires dynamic optimisation, the next step is to understand why the electrolyte composition and temperature vary and how this is linked to its actual composition. In a typical smelter with 300 - 500 cells it is historically observed that 'no two cells are the same' because of differences in start-up, and operational disturbances which alter the thermal and electrical behaviour of each cell over its lifetime. Although between-cell variation has been steadily reduced through the standardisation of cell construction, startup and operating procedures over the past ten years, between-cell variation is still important because of the large number of cells and the need to address extremes in operation as a first priority.

Despite this, variation over time within each cell is the dominant issue for electrolyte compositional and temperature control [11, 12]. This variation degrades the performance of the electrolysis through the dynamic processes described earlier. The outcomes in terms of faradaic efficiency and specific energy consumption are shown schematically in Figure 9. In the case of the faradaic efficiency in particular, the loss in efficiency is in proportion to the second derivative of the curve, or the square of the variation in the cell parameter on the abscissa [13]. Increases in specific energy consumption in Figure 9 show a similar sensitivity to variation in key parameters.

The most visible and therefore controllable part of this variation is the continually changing composition and temperature of the electrolyte. The root causes of this variation are:

i) Imbalances between energy input and energy output from the whole cell or a part of the cell. These imbalances cause freezing or melting of electrolyte - both on the cell walls and onto anodes and alumina added cold to the electrolyte. As shown in Figure 1, the phase which solidifies is cryolite, or cryolite with additives such as calcium fluoride or lithium fluoride in solid solution. However the major additives to the electrolyte are aluminium fluoride and alumina itself. Depending on the rate of freezing these components are largely rejected from the freezing interface, causing their concentration in the electrolyte to increase. Subsequent dilution of the additives then occurs during remelting of cryolite later.

ii) Compositional mass imbalances in the electrolyte caused by inappropriate additions of aluminium fluoride. These imbalances can occur if additions are made in response to concentration changes within the normal range of the variation (known as 'tampering'), rather than to the more stable rate of loss of fluoride from the electrolyte.

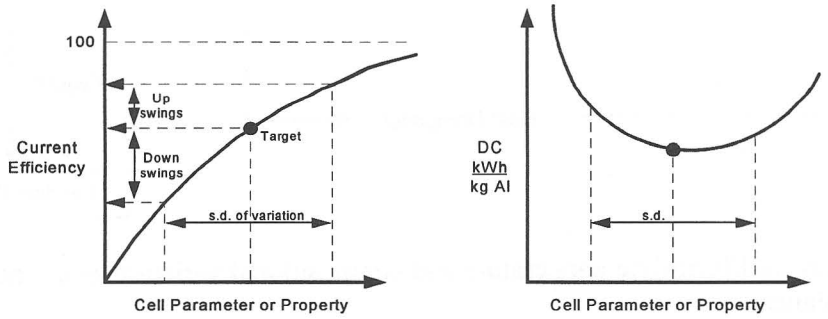

Fig. 9. Schematic showing the reduction in current efficiency and the increase in specific energy consumption caused by variation in cell parameters around their targets. Cell temperature and AlF_3 content are the most commonly measured process parameters.

Cause ii) can be eliminated using SPC techniques which prevent the inappropriate addition of aluminium fluoride. However cause i) still shifts the composition of a cell, and its operating temperature, from place to place in the temperature/composition envelope. This occurs on all smelting cells and dominates the variation when excess aluminium fluoride concentration is high, relative to the level of control of the energy balance available at the smelter.

Figure 10 investigates this mechanism more closely. Electrolyte superheat is the driving force for heat transfer from the electrolyte to the solidified sidewall ledge and to frozen electrolyte around anodes and added alumina. This driving force connects the energy balance to the compositional balance in the cell and is also responsible for the response of the operating temperature which closely follows the electrolyte liquidus point as it changes due to compositional change.

The concentration of aluminium fluoride is particularly influential in this regard because:

- Aluminium fluoride has a profound and non-linear effect on reducing the liquidus point - 3.75°C per wt % change at 10 wt % excess aluminium fluoride, but 9.6°C per wt % change at 20 wt % excess aluminium fluoride.

- As indicated earlier, aluminium fluoride is largely rejected from cryolite as it freezes into the ledge on the sidewall.

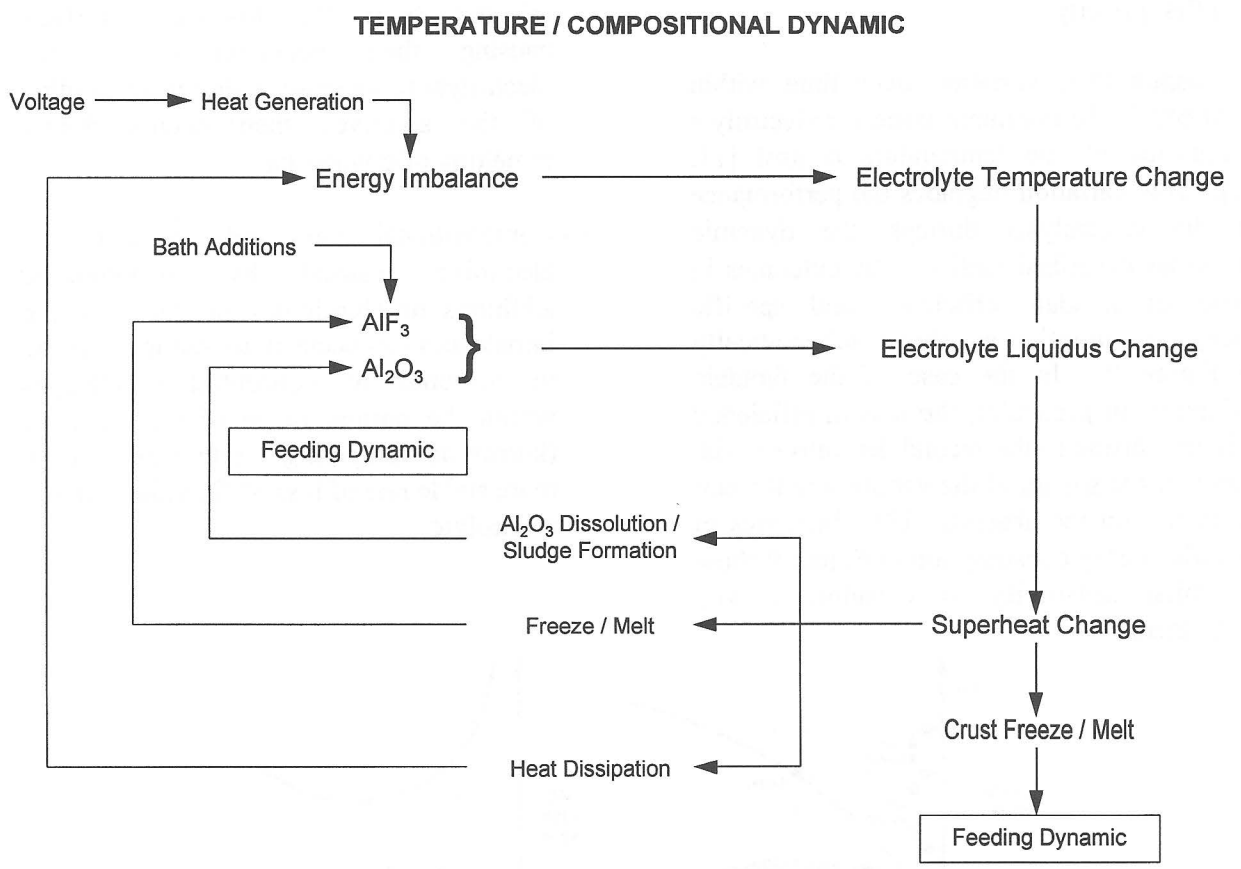

Fig. 10. Mechanism for Electrolyte temperature and compositional variation as a function of the cell energy balance.

As aluminium fluoride concentration becomes higher, the degree of change in its concentration during freezing or remelting of cryolite also increases due to the concentration process itself:

$$\frac{dC_{AlF_3}}{dt} = \frac{C_{AlF_3}}{M_{Electrolyte}} \frac{dM_{Freeze}}{dt} \qquad (3)$$

When this is combined with the non-linearity of the liquidus point relationship itself, the dual impact of AlF_3 on liquidus point dynamics is evident:

$$\frac{dT_L}{dt} = \frac{\partial T_L}{\partial C_{AlF_3}} \frac{dC_{AlF_3}}{dt} + \frac{\partial T_L}{\partial C_{Al_2O_3}} \frac{dC_{Al_2O_3}}{dt} \qquad (4)$$

where C_{AlF_3} is the excess aluminium fluoride concentration, over and above the stoichiometric amount in cryolite.

$M_{electrolyte}$ is the mass of liquid electrolyte.

M_{Freeze} is the mass of freeze, mainly cryolite

T_L is the electrolyte liquidus point

t is time

Figure 11 shows the results of equations (3) and (4) plotted for a nominated freezing rate, dM_{Freeze}/dt, of 50 kg/hour. Note that this rate of freezing is equivalent to an energy deficit of 7 kW across the smelting cell and would be typical of freezing caused by the gradual loss of insulating value of the cell's top crust over time between anode replacements (usually every 32 or 36 hours).

The rate of change of both liquidus point and aluminium fluoride concentration are shown in Figure 11 because both are important for control of the electrolyte.

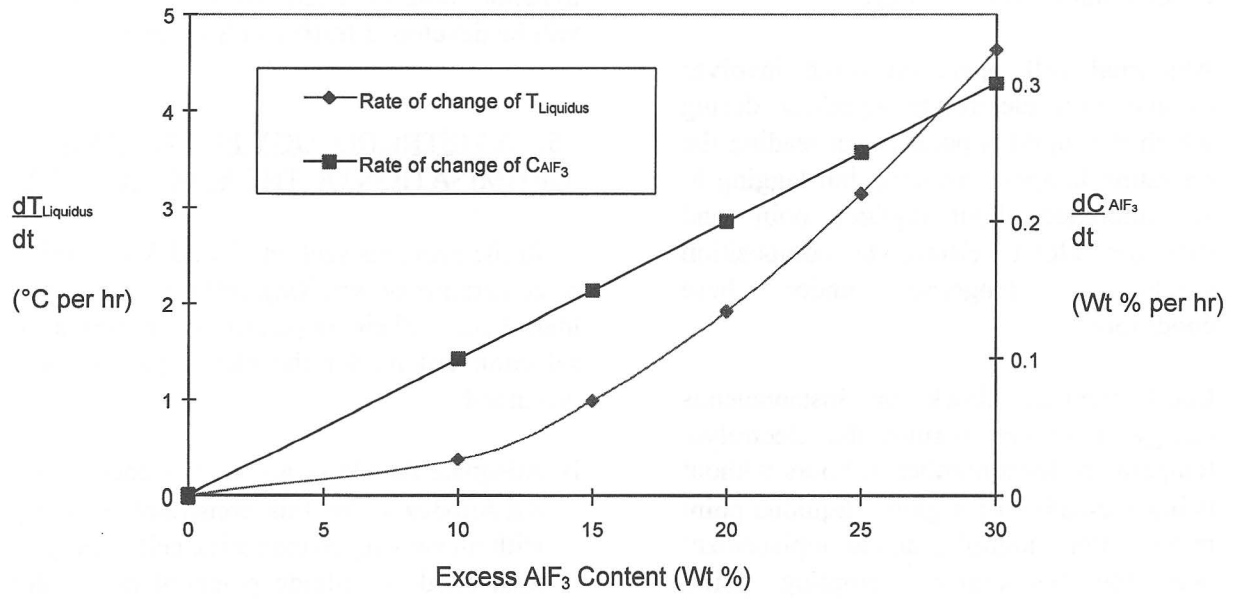

Fig. 11. Rate of change of Electrolyte liquidus point with time, for a cryolite freezing rate of 50 kg/hour and an electrolyte mass of 5000 kg.

As indicated in Figure 10, operating temperature normally follows liquidus point closely due to the self-regulating heat transfer mechanism. Operating temperature can be measured up to twice per day if necessary, with instant feedback onto runcharts or other control tools. In contrast, the aluminium fluoride concentration is difficult to sample on every cell more than once every two days and the compositional analysis is not usually available on the same day as the sample of electrolyte is taken. The time lag and gap between data points associated with aluminium fluoride concentration makes this parameter unsuitable for process control within the day to day time scale of routine cell operations. Operating temperature is a more practical control sensor in this respect but simple control action on the basis that it represents a trend in liquidus point within the cell carries a number of risks:

- A liquidus trend may be present but could conceivably be due to other electrolyte additives or to a trend in alumina concentration over 1 - 2 days.

- Abnormal cell operation often involves excursions in electrolyte superheat, during which the liquidus point is not leading the operating temperature trend but lagging it. An inference about liquidus point and therefore global electrolyte composition would be dangerous under these conditions.

- Local thermal shock or instantaneous energy input can perturb the electrolyte temperature for a number of hours without being indicative of a global liquidus point trend. For example, anode replacement near the temperature sampling point, alumina feeding or an anode effect can all lead to an operating temperature reading which is temporarily inconsistent with the overall composition and liquidus point of the electrolyte.

Given only the two sensors discussed above, it is evident that a liquidus point trend will take at least one day to detect and perhaps another two days to confirm with compositional analyses. During this first day a cell initially at 10 wt % excess aluminium fluoride and 965°C could have increased in aluminium fluoride concentration by 2.5 - 3 wt %, from Figure 11. The corresponding drop in liquidus point and operating temperature would be approximately 15°C during this period. Final operating temperature would be 950°C after a day.

If the same cell had initially been at 15 wt % excess aluminium fluoride, however, Figure 11 shows that the result would have been quite different: a 4 wt % increase in concentration and a drop in operating temperature of 30°C to give an actual operating temperature of less than 915°C after one day.

The impact of these scenarios on the electrolysis performance depends on the dynamic criteria discussed already. These will be developed further in Section 5.

5. A METHODOLOGY FOR DYNAMIC OPTIMISATION OF THE ELECTROLYTE

In the previous sections 2 and 3, a number of constraints on smelting cell operation were identified. Their implications in terms of selection criteria for the electrolyte are now discussed.

i) Adequate Anode - Cathode Distance Under All Anodes - For this constraint to apply without causing an excessive cell voltage, a total anode - cathode potential no greater than 3.3V is needed (including decomposition potential and over-potentials) in the 180,000 ampere cell discussed.

At a minimum ACD of 4.0 cm, this implies an electrical conductivity of 2.2 Ω^{-1} cm^{-1} for the electrolyte and an average alumina concentration of 3 wt % maintained in the electrolyte. To achieve this alumina concentration without large scale sludge build-up requires close control of the cell potential and at least 5°C superheat in the electrolyte at all times..

ii) Adequate Electrolyte Superheat - To prevent massive freezing of cryolite, to dissolve alumina, and to allow current draw of anodes within 12 hours of their replacement. For the 180,000 ampere cell in question, the alumina feeding system drops only 2 kg per feeder and anodes have been designed small enough to allow remelting with only 5°C superheat. Older technologies often require a higher superheat, however, because sludge back-feeding provides a significant proportion of the total alumina supply.

iii) A maximum electrolyte superheat of 15°C - To prevent complete melting of the sidewall ledge or the electrolyte components in the insulating top crust of the cell. Convective heat transfer coefficients to the ledge at the level of the electrolyte/aluminium interface are well above 1000 $W/m^2°C$ [14]. Fifteen degrees of superheat therefore requires this part of the wall to transmit a heat flux of exceeding 15,000 W/m^2 while still remaining below the electrolyte liquidus point on the internal surface of the wall. This severe duty effectively limits the average operating superheat to less than 15°C - in order to obtain adequate sidewall protection on a continuous basis. Transient superheats of greater than 20°C are observed during anode effects and also if anode failure occurs in the cell. On these occasions alumina dissolution is accelerated and alumina concentration can rise to near the saturation level for a period of time until the source of the overheating is removed.

iv) A stable electrolyte/aluminium interface - Is required to minimise back-reaction of aluminium with carbon dioxide from the anodes.

Interfacial break-up occurs above a hydrodynamic threshold which is dependent on anode - cathode distance, current density and liquid levels. The likelihood of interfacial break-up is reduced if the electrolyte has:

- Lower density
- Higher viscosity and electrolyte/metal interfacial tension

While these properties are not normally the primary drivers for interfacial break-up and poor faradaic efficiency, electrolyte conditions do exist under which they will become the drivers. The conditions are:

- High operating temperatures.
  or
- High alumina concentration.
  or
- Very low operating temperatures, often super-cooled below the liquidus point.

Under the above conditions the electrolyte/aluminium interface either becomes indistinct, due to loss of the interfacial tension (first two cases) or the electrolyte becomes more dense that the aluminium (last case) causing break-up of the liquid layers themselves.

Under any of these conditions the flux of aluminium metal back to the anodes, j_{Al}, is greater than 10% of the electrolysis rate, leading to very low faradaic efficiencies.

v) Minimum bottom sludge levels with no sludge solidification - As described earlier in Section 2.2, sludge is present in most smelting cells to some extent and this imposes a constraint on the concentration of aluminium fluoride which can be used in the electrolyte to reduce its operating temperature. When no lithium fluoride is present in the electrolyte, the maximum aluminium fluoride concentration possible is that which corresponds to an operating temperature of 945°C - the minimum solidification point of the electrolyte phase of the sludge.

Lower electrolyte temperatures than this are possible if lithium fluoride is used, however, because this additive does not segregate as strongly as aluminium fluoride. The lithium fluoride therefore reduces the liquidus points of the bulk electrolyte and the sludge phase as well. For simplicity, the electrolyte operating diagram given here assumes that lithium fluoride is not present.

The five electrolyte constraints discussed above are plotted in their most basic form in Figure 12, the axes of which are identical to those in Figure 1, although on a more detailed scale.

It is evident that the constraints define an operating region for the electrolyte within which high performance electrolysis can be obtained, provided the physical design of the cell conforms to the ACD, current density, alumina feeding, and thermal balance requirements discussed earlier. Because the electrolyte in Figure 12 is actually a quaternary system (cryolite, alumina, aluminium fluoride and calcium fluoride), the real operating envelope is multi-dimensional. However both calcium fluoride and alumina concentrations must be maintained in a tight range in order to fulfil the constraints i) - v) imposed. A two dimensional representation is therefore acceptable.

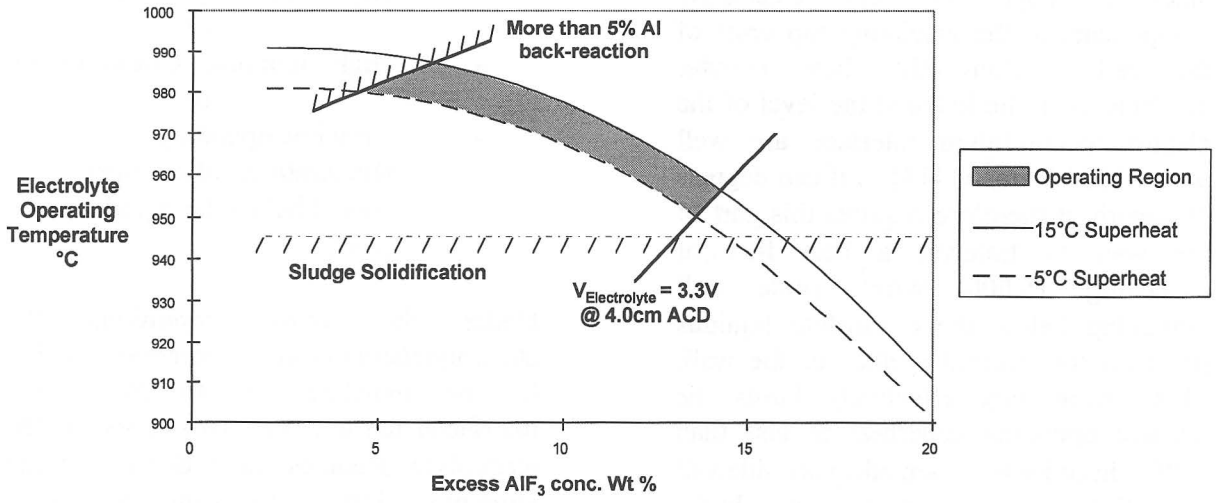

Fig. 12. Electrolyte Operating Diagram, incorporating the constraints imposed by smelting cell design and operational dynamics. Base electrolyte composition includes 0.5 wt % MgF_2, 3 wt % Al_2O_3, 5 wt % CaF_2.

The operating region in Figure 12 does not in itself define an optimum operating composition and temperature for the electrolyte. To do this it is necessary to take the controllability of the electrolyte in an industrial situation into account, as discussed in Section 4. In Figure 13 the operating region of the electrolyte is reproduced in close-up. Overlaid onto the diagram are box plots of the expected variation in temperature and excess aluminium fluoride concentration for the 10 wt % and 15 wt % aluminium fluoride starting concentrations discussed earlier.

It is evident that the 15 wt % target causes a significant (perhaps 50%) proportion of the cell's operating life to be spent outside the lower two constraints of the operating region - constraints (i) and (v). As indicated on the diagram this will bring about other abnormalities in the cells operation associated with the build-up and solidification of sludge, the failure of anodes through low ACD and/or contact with this material, and numerous other by-products of high superheat excursions.

The above methodology can be refined further, and supplemented by more data on the controllability of the electrolyte in practice, in order to locate the optimum composition for a particular cell design or to test the effect of a new electrolyte additive to the system.

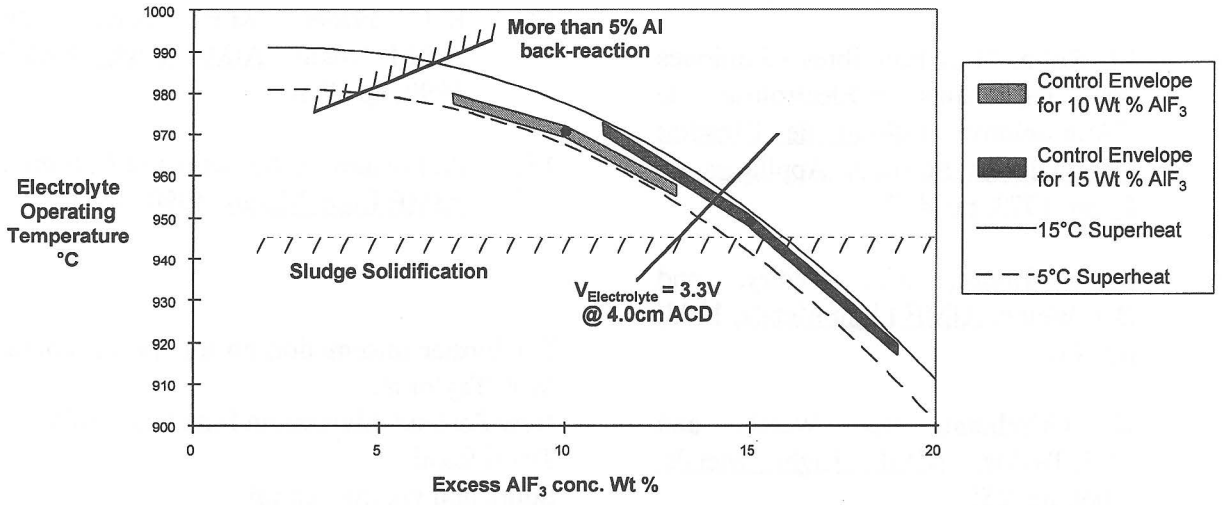

Fig. 13. Electrolyte operating diagram with electrolyte controllability overlaid

REFERENCES

1. K. Grjotheim, C. Krohn, M Malinovský, K Matiašovský, and J. Thonstad, Aluminium Electrolysis, Fundamentals of the Hall-Héroult Process, Aluminium-Verlag, 2nd Edition, 1982.

2. K. Grjotheim and B.J. Welch, Aluminium Smelter Technology, Aluminium-Verlag, 2nd Edition, 1988.

3. W.D. Zhang, J.J.J. Chen, M.P. Taylor, and B.J. Welch, Chemica 91, Proceedings of 19th Australasian Chemical Engineering Conference, Newcastle, Australia, 1991, pp. 721.

4. M. Rolin, "Les Equilibres Chimiques dan les bains d'Electroluse de l'Aluminium", Edition de l'Institut National des Sciences Appliques de Lyon, 1973, pp. 497.

5. M.P. Taylor, J.T. Keniry, and B.J. Welch, AIME Light Metals, 1983, pp. 437.

6. K. Grjotheim, B.J. Welch, and M.P. Taylor, AIME Light Metals, 1989, pp. 255.

7. M.P. Taylor, X. Liu, K.J. Fraser, and B.J. Welch, AIME Light Metals, 1990, pp. 259.

8. W. Haupin, "The Influence of Additives on Hall-Héroult Bath Properties", Journal Of Metals, November 1991, pp. 28.

9. W. Haupin, and Helge Forberg, Light Metal Age, 1995, pp. 40.

10. P. Fellner,and A. Silny, "Viscosity of Sodum Cryolite-Aluminium Fluoride-Lithium Fluoride Melt Mixtures", Ber. Bunsenges. Phys. Chem, Vol. 98, 1994, pp. 935-937.

11. R. Stone, and M.P. Taylor; The Statistician, Vol. 44, No. 2, 1995, pp. 227 - 234

12. M.P. Taylor, W.D. Zhang, S. Schmidt, and V.Wills, Trans. I. Chem. E, November 1996, in press.

13. F.J. Stevens, W.D. Zhang, M.P. Taylor, and J.J.J. Chen, AIME Light Metals, 1992, pp. 541.

14. K.J. Fraser, M.P. Taylor, and A.J.M. Jenkin, AIME Light Metals, 1990, pp. 221.

15. A. Rostum, A. Solheim and A. Sterten, AIME Light Metals, 1990, pp. 311.

For further information on this paper, contact M.P. Taylor at:
New Zealand Aluminium Smelters Limited
Tiwai Road,
Southland via Invercargill,
New Zealand.

Telephone: 64 3 218 5023
Facsimile: 64 3 218 5017